Journal of Neurochemistry

JOURNAL OF NEUROCHEMISTRY | 2020 | 152 | 710–726

doi: 10.1111/jnc.14870

ORIGINAL ARTICLE

Quantitative proteomics of synaptosome *S*-nitrosylation in Alzheimer's disease

Teodora Stella Wijasa*, Marc Sylvester†, Nahal Brocke-Ahmadinejad†, Stephanie Schwartz‡, Francesco Santarelli*, Volkmar Gieselmann†, Thomas Klockgether*§, Frederic Brosseron*[1] and Michael T. Heneka*‡[1]

*German Center for Neurodegenerative Diseases (DZNE), Bonn, Germany

†Institute of Biochemistry and Molecular Biology, University of Bonn, Bonn, Germany

‡Department of Neurodegenerative Diseases and Geriatric Psychiatry, University Hospital Bonn, Bonn, Germany

§Department of Neurology, University of Bonn, Bonn, Germany

Abstract

Increasing evidence suggests that both synaptic loss and neuroinflammation constitute early pathologic hallmarks of Alzheimer's disease. A downstream event during inflammatory activation of microglia and astrocytes is the induction of nitric oxide synthase type 2, resulting in an increased release of nitric oxide and the post-translational S-nitrosylation of protein cysteine residues. Both early events, inflammation and synaptic dysfunction, could be connected if this excess nitrosylation occurs on synaptic proteins. In the long term, such changes could provide new insight into patho-mechanisms as well as biomarker candidates from the early stages of disease progression. This study investigated S-nitrosylation in synaptosomal proteins isolated from APP/PS1 model mice in comparison to wild type and $NOS2^{-/-}$ mice, as well as human control, mild cognitive impairment and Alzheimer's disease brain tissues. Proteomics data were obtained using an established protocol utilizing an isobaric mass tag method, followed by nanocapillary high performance liquid chromatography tandem mass spectrometry. Statistical analysis identified the S-nitrosylation sites most likely derived from an increase in nitric oxide (NO) in dependence of presence of AD pathology, age and the key enzyme NOS2. The resulting list of candidate proteins is discussed considering function, previous findings in the context of neurodegeneration, and the potential for further validation studies.

Keywords: Alzheimer's disease, mass spectrometry, neuroinflammation, S-nitrosylation, synaptosome.

J. Neurochem. (2020) **152**, 710–726.

Various studies have demonstrated the relationship between cognitive impairment and synaptic dysfunction in the early stages of Alzheimer's Disease (AD) (Tomiyama *et al.* 2010; Hammerschmidt *et al.* 2013; Swomley *et al.* 2014; Tonnies and Trushina 2017). Area-specific decreases in synaptic density can be found in the AD brain (DeKosky and Scheff 1990; Terry *et al.* 1991), e.g., in the temporal and frontal cortex (Davies *et al.* 1987). Even when synapses seem structurally intact, they may be dysfunctional (Yao *et al.* 2003). These slight alterations may account for the earliest symptoms of AD, which may occur years before the clinical diagnosis of dementia is made (Boyd-Kimball *et al.* 2005; Chang *et al.* 2013). Therefore, it can be hypothesized that this "preclinical" AD phase provides an opportunity for therapeutic intervention, and therefore biomarkers of this

Received April 25, 2019; revised manuscript received August 23, 2019; accepted September 4, 2019.

Address correspondence and reprint requests to Michael T. Heneka, German Center for Neurodegenerative Diseases (DZNE), Clinical Neuroscience Unit, University Hospital Bonn, Sigmund-Freud-Str. 25, 53127 Bonn, Germany. E-mail: michael.heneka@ukbonn.de

[1]These authors contributed equally to this work.

Abbreviations used: AD, Alzheimer's disease; Aβ, amyloid beta; CSF, cerebrospinal fluid; EEF2, elongation factor 2; FHL1, four and a Half LIM domains protein 1; GSTM3, glutathione S-transferase Mu 3; HSDL1, hydroxysteroid dehydrogenase-like protein 1; IodoTMT, iodoacetyl tandem mass tag; Limma, linear models for microarray data; MCI, mild cognitive impairment; MOG, myelin-oligodendrocyte glycoprotein; NCAN, neurocan core protein; NDRG2, N-myc downstream-regulated Gene 2 protein; NDUFAB1, NADH:ubiquinone oxidoreductase subunit AB1; NO, nitric oxide; NOS2, nitric oxide synthase type 2; RP, rank product; ranks of fold change; RRID, research resource identifier (see scicrunch.org); SDHA, succinate dehydrogenase [ubiquinone] flavoprotein subunit, mitochondria; SLC1A3, excitatory amino acid transporter 1; SLC30A3, Zinc transporter 3; SNO, S-nitrosylation; WT, wild-type.

disease stage should be further investigated (Sperling *et al.* 2011; Fiandaca *et al.* 2014).

Neuroinflammation occurs alongside neurodegenerative processes and plays a key role in the development of AD (Agostinho *et al.* 2010; Meraz-Ríos *et al.* 2013; Heneka *et al.* 2015). Neuroinflammation has been shown to lead to the release of pro- and anti-inflammatory mediators and induction of pro-inflammatory enzymes, including nitric oxide synthase 2 (NOS2) and prostaglandin synthase 2.

Cytokine-induced NOS2 expression causes post-translational protein modifications through the sustained generation of NO, which can be taken as a fingerprint of neuroinflammatory activity in the brain (Heneka and Feinstein 2001; Colton *et al.* 2008). Increased levels of nitrated proteins have been reported in the brain and cerebrospinal fluid (CSF) of patients with AD, indicating a sustained activity of NOS2 in the central nervous system (Nakamura *et al.* 2013; Seneviratne *et al.* 2016).

Under physiological conditions, there are two NOS enzymes that are expressed constitutively: neuronal nNOS/ NOS1 and endothelial eNOS/ NOS3 (Förstermann and Sessa 2012). One of the key biological modifications induced by NO is the S-nitrosylation (SNO) of cysteine residues. This modification is reversible and plays an essential role in NO signaling (Nakamura *et al.* 2013). Proteins that have been nitrosylated vary in their response to this modification; resulting in either their activation or inactivation. S-nitrosylation participates in a variety of physiological processes, including the regulation of cell signal transduction pathways, conformational changes, protein–protein interaction, and cell survival (Shi *et al.* 2013).

In contrast, inflammation-induced iNOS/ NOS2 expression can result in abnormal levels of S-nitrosylation and thereby cause cellular dysfunction and neurodegeneration (Nakamura and Lipton 2016). Studies carried out in NOS2 knockout mice have shown a correlation between NOS2, amyloid beta (Aβ) deposition, and cognitive dysfunction in AD mouse models (Colton *et al.* 2008; Kummer *et al.* 2011). The SNO-proteome in cortex and hippocampus tissues is altered in both the CK-p25 mouse model of AD and the P301S mouse model of tauopathy (Seneviratne *et al.* 2016; Amal *et al.* 2019).

In this study, our aim was to characterize the NOS2-dependent SNO of synaptic proteins as a fingerprint of neuroinflammation in mouse and human brain samples to discover new potential biomarker candidates for AD. Mass spectrometry-based quantification with an irreversible Cys-reactive reagent of Iodoacetyl Tandem Mass Tag (IodoTMT™, Thermo Fisher Scientific, Waltham, MA, USA) was used for both mice and human studies (Wijasa *et al.* 2017). The age effect and genotype effect were analyzed in synaptosome samples prepared from wild-type (WT) and AD-transgenic mice. Data obtained from murine AD models were then compared with brain samples from AD, mild cognitive impairment (MCI), and healthy elderly subjects.

Methods

Animals

All animals and experiments were maintained according to the legal and ethical requirements of the University of Bonn – Medical Center (Germany) and the North Rhine-Westphalia (NRW) federal ministry for nature, environment and consumer protection (Landesamt für Natur, Umwelt und Verbraucherschutz Nordrhein-Westfalen, LANUV). Mice were housed for brain preparation only which did not require further approval. An overview of the mice study design and samples is provided in Fig. 1 and Table 1. Four age-matched male transgenic mice groups were used in this study, maintained on C57BL/6J genetic background. They were obtained from the Jackson Laboratories and breed internally. APP/PS1$^{+/-}$ mice (RRID:IMSR_JAX:34832-JAX) were studied as AD model with C57BL/6J wild type (WT) (RRID:IMSR_JAX:000664) as controls. NOS2$^{-/-}$ mice (RRID:IMSR_JAX:002609) were used to test the role of NOS2-derived NO in neuroinflammation. APP/PS1$^{+/-}$ was bred with NOS2$^{-/-}$ mouse in-house to generate the litters in one of the groups used in this study. Deletion of inducible NOS in an APP/PS1 background (APP/PS1/NOS2$^{-/-}$) was used to identify protein SNO sites related to neuroinflammation in AD. DNA isolation was performed from a small piece of tail of the offsprings of APP/PS1/NOS2$^{-/-}$. Mice were genotyped by polymerase chain reaction using the following primers (RRID:SCR_006898): PrP-Antisense: agcctagaccacgagaatgc, 237F: caggtggtggagcaagatg, S36: ccgagatctctgaagtgaagatggatg, BACE HC69: aggcagctttgtggagatggtg, BACE HC70: cgggaaatggaaaggctactcc. APP band was expected at 400 base pairs (bp), PS1 band was at 1.2 kilobases (kb) and no band for NOS2$^{-/-}$. For genotype identification, the APP/PS1$^{+/-}$ tail was used as a positive control and NOS2$^{-/-}$ as a negative control. Each tail sample was digested with 5 μL of proteinase K in 1 mL of lysis buffer (containing in mM: 50 Tris-HCl, 50 KCl, 2.5 EDTA pH 8.0, 0.45% NP-40 and 0.45% tween 20) and left overnight at 55°C with agitation (650rpm on a heated shaker). DNA samples were vortexed and centrifuged to pellet the debris. DNA precipitates were dissolved in 100 μL of distilled water. For the amplification reaction, 1 μL of DNA (or water in the negative control) was added to 19 μL of PCR mix containing 10 μM of primers in a total reaction volume of 20 μL. Samples were denaturated at 95°C for 3 min and then subjected to 35 cycles of 95°C for 30 s (s), 65°C for 75 s and 72°C for 60 s, with a final extension step of 4 min at 72°C and paused at 4°C. PCR products were separated on a 2% agarose gel electrophoresis (120 V for 30 min) and photographed for documentation.

Mice were housed in groups under standard conditions at 22°C and a 12 h light–dark cycle with free access to food and water. At 3 months or 12 months, animals were anesthetized using isoflurane and transcardially perfused, using ice-cold normal saline immediately before synaptosome isolation. Isoflurane inhalation was used due to short induction, minimal handling, and the reliability of its effects. Animal numbers were $n = 20$ per each group (in total 160 mice from 8 groups). Whole brain hemispheres (without cerebellum and brainstem) were used for protein extraction. The mice were arbitrary assigned for the brain collection. Blinding was not performed. Animal handling procedures were conducted according to the NIH Guide for the Care and Use of Laboratory Animals.

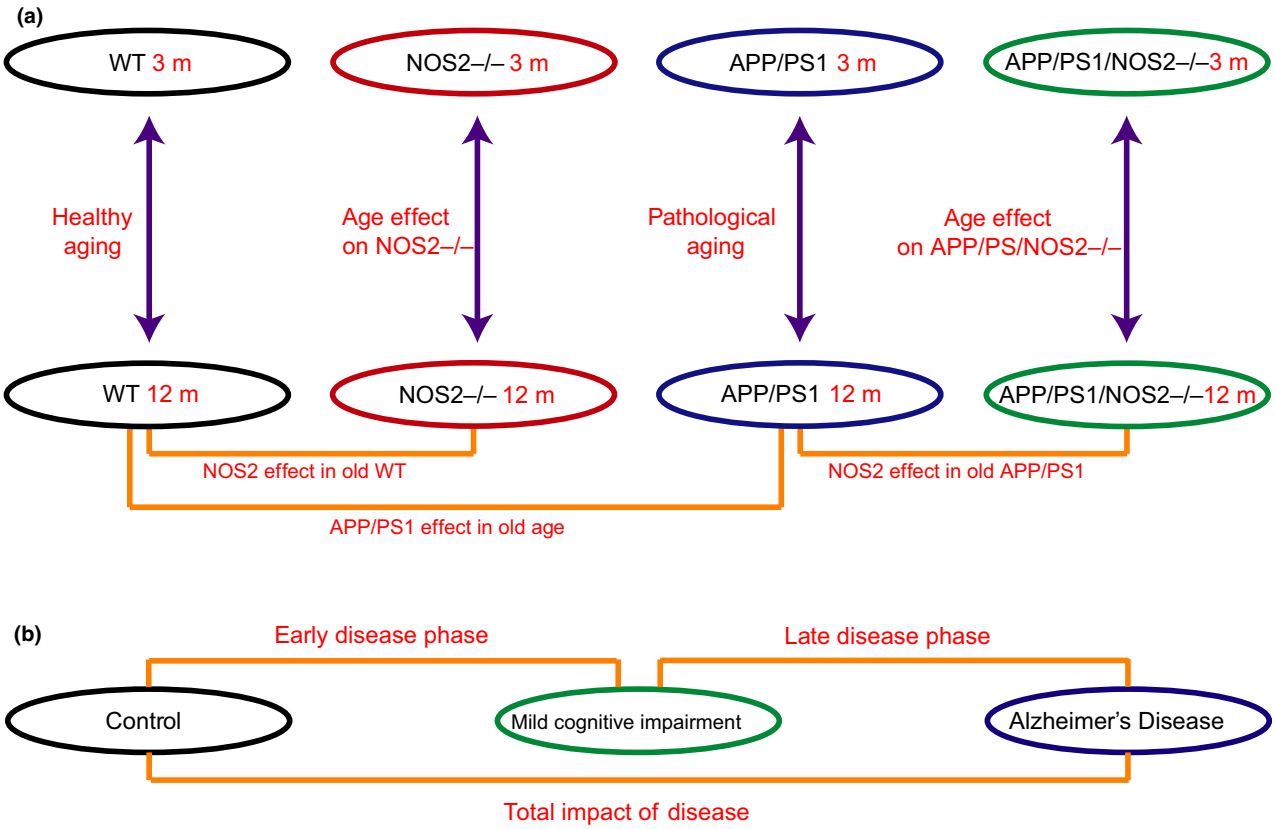

Fig. 1 Overview of group-wise comparisons used in mouse and human samples. (a) Murine synapto-SNO-proteomes were examined by a series of comparisons to differentiate age-dependent, APP/PS1-dependent and NOS2-dependent effects. The experimental groups (n = 12 each) were 3-month and 12-month-old wild type (WT), $NOS2^{-/-}$ (NOS2 knockout mice, NOS2ko), APP/PS1 (transgenic mice carrying the human APP and presenilin1 gene) and APP/PS1/$NOS2^{-/-}$ (transgenic mice carrying the human APP, presenilin1 gene crossed with $NOS2^{-/-}$). (b) Human synapto-SNO-proteomes were examined by disease stage-based comparison.

Human sample material

All human brain samples were provided from clinically and pathologically well-characterized cases at Banner Sun Health Research Institute Brain and Body Donation Program (BBDP) in Sun City, Arizona (Beach *et al.* 2015). All subjects participating in the Banner Brain and Body Donation Program signed a written informed consent. The BBDP has been approved by the institutional review board and research conducted on BBDP subjects is carried out in accordance with The Code of Ethics of the World Medical Association (Declaration of Helsinki) for experiments involving humans. Frozen human cortical brain tissues were collected postmortem (n = 30 healthy control, n = 30 MCI and n = 30 AD). These three groups were matched with regard to age, sex, and postmortem interval of less than 4 h (Table 1). Diagnoses were made according to the neuropathologic diagnosis of AD, known as the National Institute on Aging/Reagan Institute of the Alzheimer Association Consensus Recommendations for the Postmortem Diagnosis of AD or NIA-Reagan Criteria. Specifically, tissues were assessed for Aβ plaque score, Braak neurofibrilliary tangles stage, and CERAD neuritic plaque score were assigned to each sample, indicating possible AD, or definite AD. Blinding was not performed.

Synaptosome isolation

Synaptosomes were purified as described previously (Wijasa *et al.* 2017). In brief, synaptosomes were isolated from mouse and human brain samples and directly placed in a Teflon-glass homogenizer with ninefold volume of tissue weight in ice-cold 0.32 M sucrose (consists of 50 mM Tris-Acetat, 1 mM EGTA, 1 mM EDTA, 1 mM AEBSF, cOmplete protease inhibitor cocktail 0.2% V/V, 5 mM $Na_2H_2P_2O_7$, 5 mM NaF, 2 mM $NaVO_3$, pH 7.4). Homogenates were cleared by centrifugation at 800 g for 5 min. The pellet was discarded and the supernatant was layered on top of a discontinuous sucrose density gradient consisting of 1.0 mol/L and 1.4 mol/L sucrose buffer and centrifuged at 54 000 g in a swinging bucket rotor (Optima™ MAX-XP ultracentrifuge, Beckman Coulter, Brea, CA, USA) for 90 min. Purified synaptosomes were collected at the interface between 1.0 M and 1.4 M sucrose. The resultant fraction was diluted with fourfold volume of HPLC-grade water and pelleted at 54 000 g for 15 min. The supernatant was discarded and the synaptosomal pellet was stored immediately at −80°C. The quality of the synaptosome purification was performed using a 3-month-old WT mice and healthy control human samples (n = 3/ group) by immunoblotting against synaptic, cytosolic, and nuclear markers. Equal amounts of protein samples (20 µg) were

Table 1 Overview on sample and subject features

Species	Feature	Experimental group			
		WT	$NOS2^{-/-}$	APP/PS1	APP/PS1/$NOS2^{-/-}$
Mouse	Age (mth.)	3 and 12	3 and 12	3 and 12	3 and 12
	Sex (% male)	100	100	100	100
	Sample size (n)	20	20	20	20
	Sample size (n) after QC	12	12	12	12

	Feature	CON	MCI	AD	Significance
Human	Age (yrs.)	87.4 ± 8.173–99	92.1 ± 7.283–99	84.3 ± 10.166–99	All: 0.013MCI Vs. AD 0.015
	Sex (% male)	57	50	53	All: 0.875
	PMI (h)	2.8 ± 0.71.5–3.8	2.7 ± 0.71.8–3.5	2.6 ± 0.61.5–3.5	All: 0.922
	MMSE	28.5 ± 1.426–30	26.7 ± 2.521–30	11.9 ± 9.80–28	All: $2x10E^{-8}$CON vs. AD 2 × $10E^{-8}$MCI vs. AD 8 × $10E^{-5}$
	ApoE	3/3	3/3	3/4	All: 2 × $10E^{-5}$CON vs. AD 2 × $10E^{-5}$MCI vs. AD 3 × $10E^{-3}$
	Braak Stage	2.7 ± 1.01–4	3.2 ± 1.11–5	5.4 ± 0.74–6	All: 5 × $10E^{-13}$CON vs. AD 5 × $10E^{-12}$MCI vs. AD 3 × $10E^{-8}$
	Sample size (n)	30	30	30	
	Sample size (n) after QC	20	20	20	

This study used brain tissue from mice and human subjects. Sample sizes were kept identical for all groups, including after quality control (QC) of the mass spectrometry data. In the mice part of the study, the experimental groups were male 3-month and 12-month-old wild type (WT), $NOS2^{-/-}$ (NOS2 knockout mice, NOS2ko), APP/PS1 (transgenic mice carrying the human APP and presenilin1 gene) and APP/PS1/$NOS2^{-/-}$ (transgenic mice carrying the human APP, presenilin1 gene crossed with $NOS2^{-/-}$). For the human part of the study, features of samples and sample donors are described as mean ± standard deviation plus range. For APOE genotype, the most frequent genotype is reported. For MMSE, the last available testing data were used. Group comparisons were done using ANOVA or Chi^2 test. Results are reported for all groups and for significant adjusted pairwise comparisons. By tendency, MCI patients were slightly older than control or AD patients, which made a significant difference between MCI and AD groups. There was no significant difference in sex or postmortem interval (PMI) between the groups. In accordance to AD pathogenesis and clinic, AD patients showed significantly reduced cognitive performance, a higher frequency of ApoE4 alleles, and had progressed further in the Braak staging scheme.

separated by 4–12% NuPAGE (Invitrogen), using MES buffer and transferred to the nitrocellulose membranes. Membranes were incubated for 30 min at room temperature in blocking solution (20 mM Tris, 150 mM NaCl, and 3% w/v bovine serum albumin/BSA), followed by incubation at 4°C overnight with primary antibodies in TBS-T (20 mM Tris, 150 mM NaCl, 3% w/v bovine serum albumin/BSA, and 0.1% tween-20). Immunoblots were performed using the following primary antibodies: rabbit anti-synaptophysin (1 : 1000, Abcam, ab52636, RRID AB_882786, Cambridge, UK), rabbit anti-NMDA receptor 2B (NMDAR2B, 1 : 1000, Millipore Corporation, Burlington, MA, USA, ab1557p, RRID AB_11214394), rabbit anti-glutamate receptor 1 (GluA1, 1 : 1000, Millipore, ab1504, RRID AB_2113602), mouse anti-post-synaptic density protein (PSD95, 1 : 2000, Thermo Fisher Scientific, MA1-064, RRID AB_2092361), mouse anti-nuclear antigen Lamin B1 (1 : 500, Proteintech, 66095-1-Ig, RRID AB_11232208) and mouse anti-alpha tubulin (1 : 2000, Thermo Fisher Scientific, 62204, RRID AB_1965960). Further reagents and resources are described in the supplementary material.

IodoTMT labeling and mass spectrometry

All chemicals and antibodies used in this study are listed in detail in the supplementary file methods section. Isobaric mass tag labeling using iodoTMT™ (Thermo Fisher Scientific), nanocapillary high-performance liquid chromatography tandem mass spectrometry, and basic mass spectrometry data processing were performed as previously described (Wijasa *et al.* 2017). The identified proteins were annotated using Uniprot/SwissProt database (Bateman *et al.* 2015) and then classified using Panther Gene Ontology (GO) (Thomas *et al.* 2003) and Gorilla search engine (Eden *et al.* 2009). Identified SNO sites were compared to entries in a S-nitrosylation database (http://dbSNO.mbc.nctu.edu.tw). Further reagents and resources are described in the supplementary material.

Statistics and data analysis

Since we did not have information about the predicted variables, the sample size was not calculated before. Statistical analysis followed the same workflow and parameters for the mice and human data sets, respectively. Peptide mass spectrometry intensities were log2 transformed to approximate normal distribution and enable parametric testing. Next, a pairwise Pearson correlation matrix was calculated for all internal standard samples of each data set. If the Pearson correlation score of a single mass spectrometry sixplex run was below 0.5, all samples of this run were excluded from further analysis as a quality control of the TMT-labeling procedure.

After this quality control, a series of inter-group pairwise tests was conducted: In the mice data set, each genotype was contrasted against each other and across age (3 months vs 12 months old). On

human results, pairwise tests were performed in which each group of patients was compared to each other. To minimize false positive results, the peptides identified in less than 50% of the total biological replicates were omitted (Kuster *et al.* 2005; Blonder and Veenstra 2007; Mallick *et al.* 2007).

To identify regulated peptides/proteins, a combination of Linear Models for Microarray Data (limma), Rank Product (RP), and bootstrap analysis was used. TMT tag reporter ion intensities were used to calculate fold change using limma and RP (Schwammle *et al.* 2013). P-values were calculated for each peptide and adjusted for multiple testing, using the Benjamini and Hochberg approach to control false discovery rates. Additionally, random sampling with replacement (bootstrap analysis) was calculated to evaluate if the initial fold change was representative of the population (Mukherjee *et al.* 2003; Wang *et al.* 2012; Zhang *et al.* 2016). The bootstrap analysis for the identification of differently expressed proteins in this study was performed using 10000 permutations. Proteins were considered significant if adjusted p-values (limma q-value and/ or RP q-value) were below the significance level $\alpha = 0.05$ and/ or if the protein was within the 95% confidence interval (CI) of the bootstrap analysis. The fold–change threshold was set to a minimum 1.2-fold. To reduce false positives, proteins with lower fold change were excluded even when otherwise within significance criteria. To globally visualize the data of the intergroup pairwise comparisons, log2 fold change of each SNO-Cys protein was plotted against –l og2 adjusted p-value in a volcano plot. Venn diagrams were calculated using a freely available web tool (Venny 2.1., Oliveros, 2007-2015) on the protein level excluding duplicate protein entries.

Further evaluation was focused on those SNO-peptides for which an increase was observed under pathological conditions, as disease relevant neuroinflammatory processes would always result in increased release of NO.

Results

Quality control & basic features of the data set

Protein yields obtained from the purified synaptosomes were comparable between mouse and human samples (3.0 ± 1.0 μg/mg and 2.8 ± 0.8 μg/mg, respectively). The purity of synaptosome isolations was analyzed by western blot detection of specific synaptic and nuclear markers, using brain samples from 3-month-old WT mice and healthy human controls (Figure S2). In accordance with successful isolation of synaptosomes, pre- and post-synaptic proteins including synaptophysin, NMDAR2B, GluA1, and PSD95 were enriched in the synaptosomal fraction compared with whole brain tissue homogenates, while the nuclear marker Lamin B1 was depleted in the synaptosomes relative to whole brain tissue homogenates.

By inter-run quality control of the mass spectrometry sixplex internal standards, 60% of the murine samples ($n = 12$ per group) and 67% of the human samples ($n = 20$ per group) were included in statistical analysis. Descriptive data on the biological/ clinical features of the mouse and human specimen is provided in Table 1.

Of the SNO sites found in the proteomics data, 33% of the murine and 69% of the human modification sites were identified for the first time based on comparison to a S-nitrosylation database (http://dbSNO.mbc.nctu.edu.tw).

S-nitrosylation of synaptic proteins in AD mouse model

To identify those proteins with an increase in SNO in an age-, pathology- and NOS2-dependent manner, a series of pairwise comparisons were performed (see Fig. 1 for an overview). First, we tested the age effect within each individual genotype group (old 12 month compared with young 3-month-old mice, Fig. 2 and Table S1), and then the genotype effect between the 12-month-old mice groups (Fig. 3 and Table S2) was tested.

The first comparison was between old and young WT mice to identify changes in SNO related to physiological aging (Fig. 2a). A total of 434 synapto-SNO proteins were detected. Of these, 101 proteins were significantly increased. The comparison of old and young APP/PS1 mice indicated pathological aging (Fig. 2c), which yielded a total of 429 SNO proteins from the APP/PS1 samples (AD mouse model). Of these, 87 SNO proteins were significantly increased.

To determine which of these 87 SNO proteins were modified in a NOS2-dependent manner, the same analysis was repeated comparing the synapto-SNO proteome between old and young $NOS2^{-/-}$ and APP/PS1/$NOS2^{-/-}$ transgenic mice (Fig. 2b, d). This detected 431 SNO proteins from the $NOS2^{-/-}$ samples, of which 53 SNO proteins were increased significantly. Similarly, of the 444 SNO proteins that were identified during aging in the APP/PS1/$NOS2^{-/-}$ samples, 58 SNO proteins were significantly increased. It was postulated that non-overlapping synapto-SNO proteins that were only detected in APP/PS1-derived samples could show NOS2-dependent proteins that are directly related to the neuroinflammatory processes observed in APP/PS1 mice. There were 17 SNO proteins that fulfilled these criteria (Fig. 4a).

To visualize the effects of APP/PS1 and NOS2 gene deletion in 12-month-old mice (genotype effect), Venn diagrams were generated using three pairwise group comparisons (Fig. 3). WT was compared with $NOS2^{-/-}$ at the same age in order to identify the effect of NOS2 gene deletion on the WT background. A total of 460 SNO proteins were identified and of these, 32 SNO proteins were identified as significantly increased. Next, APP/PS1 was compared with APP/PS1/$NOS2^{-/-}$ to identify which SNO modifications are NOS2-dependent. This yielded a total of 467 SNO proteins, of which 45 SNO proteins met the significance criteria. Finally, APP/PS1 mice were compared with WT mice to delineate the SNO modifications that occur due to cerebral amyloidosis. In APP/PS1 compared with WT samples 465 SNO proteins were found, of which 39 SNO proteins were significantly increased.

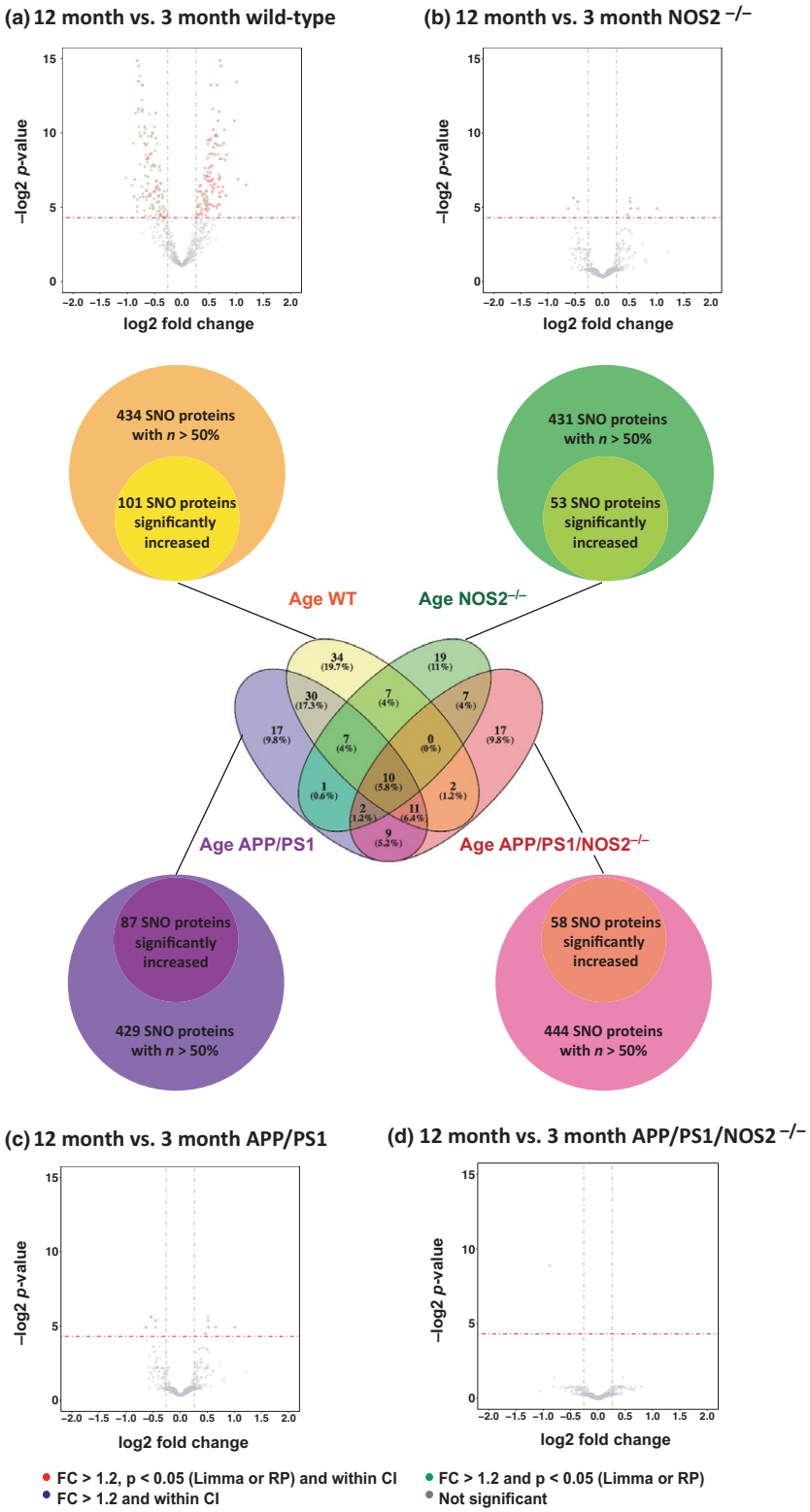

Fig. 2 Distribution of proteomics data in age-dependent comparisons. To investigate the age effect, synapto-SNO-proteome data was compared between of old (12 month) against young (3 month) mice. (a) A total of 434 synapto-SNO proteins in wild-type samples were identified. Of these, 101 proteins were significantly increased. (b) In NOS2$^{-/-}$samples 431 SNO proteins were identified, of which 53 SNO proteins were significantly up-regulated. (c) The comparison of old and young APP/PS1 mice yielded a total of 429 SNO proteins from the APP/PS1 samples (AD mouse model). Of these, 87 SNO proteins fulfilled the significance criteria. (d) Of 444 SNO proteins identified in the APP/PS1/NOS2$^{-/-}$ samples, 58 SNO proteins were significantly up-regulated. In volcano plots, negative $\log_2$ p-values (adjusted Limma p) were plotted against $\log_2$ protein fold change values. Dotted lines indicate the minimum fold change (grey lines) and *p*-values (orange) considered significant.

There were six SNO proteins that increased in both analyses, aged APP/PS1 vs aged APP/PS1/NOS2$^{-/-}$ and aged APP/PS1 vs aged WT mice. Five of these SNO proteins were modified by NO in response to cerebral amyloidosis (Fig. 4b). The results further revealed four overlapping proteins when corrected for age- and genotype-dependent

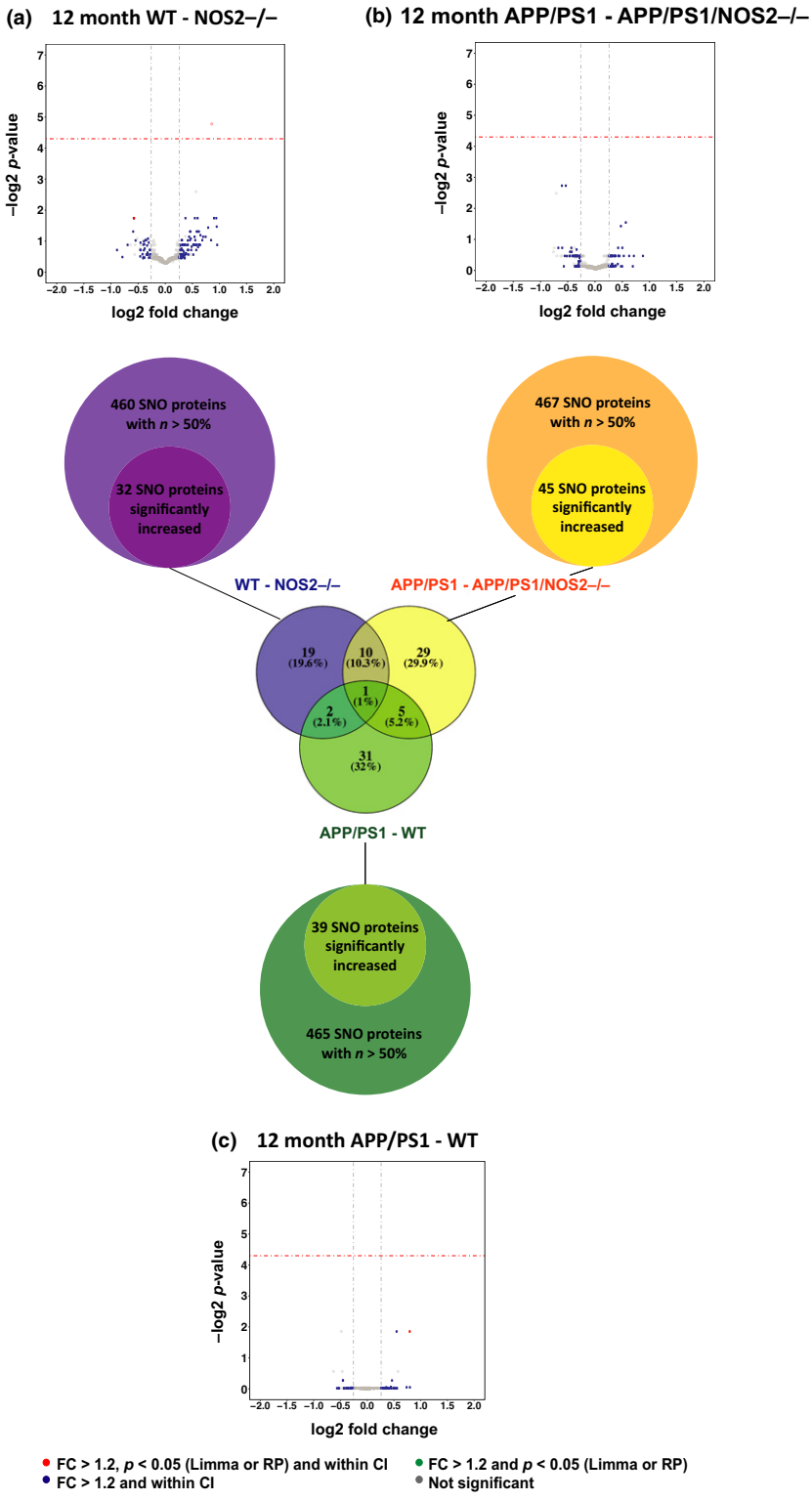

Fig. 3 Distribution of proteomics data in genotype-dependent comparisons. To determine the genotype effect in 12-month-old mice, synapto-SNO-proteome data was compared between genotypes of 12-month-old age-matched animals. (a) 460 SNO proteins were included in the comparison of WT vs. $NOS2^{-/-}$ samples. Of these, 32 proteins were significantly up-regulated. (b) Comparison of 12-month APP/PS1 vs. APP/PS1/$NOS2^{-/-}$ samples (467 SNO proteins included, 45 up-regulated in WT). (c) APP/PS1 vs. WT samples (465 SNO included, 39 up-regulated). In volcano plots, negative $\log_2$ p-values (adjusted Limma p) were plotted against $\log_2$ protein fold change values. Dotted lines indicate the minimum fold change (grey lines) and p-values (orange) considered significant.

effects: n-myc downstream-regulated gene 2 protein (NDRG2), NADH:ubiquinone oxidoreductase subunit AB1 (NDUFAB1), excitatory amino acid transporter 1 (SLC1A3), and inactive hydroxysteroid dehydrogenase-like protein 1 (HSDL1) (Fig. 4c). The list of NOS2-dependent SNO proteins up-regulated by aging and/ or APP/PS1 genotype mice is shown in table 2.

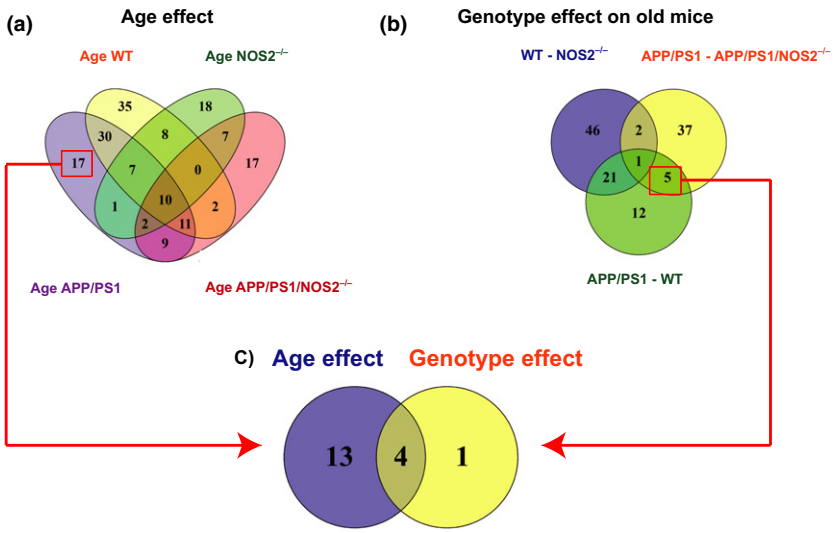

Fig. 4 Overlap of increased proteins between age and genotypes. (a) The diagrams differentiate synapto-SNO proteins that were increased in an age-dependent manner. A total of 17 proteins were found to increase during aging in a NOS2-dependent manner specifically in APP/PS1 mice. (b) Synapto-SNO proteins that were increased in APP/PS1 mice and are NOS2-dependent (5 selected proteins). (c) Overlap between NOS2-dependent synapto-SNO proteins increased in age-dependent and/or APP/PS1 genotype-dependent manner. These proteins could provide primary candidates for validation (see Table S4).

Functional classification of nitrosylated murine proteins

To further understand the functional impact of NOS2-mediated protein nitrosylation, an analysis of associated Gene Ontology terms was performed using the Panther database (http://pantherdb.org) "PANTHER version 13.1 Released 2017-04" at $p < 0.05$ (Fig. 5) (Thomas *et al.* 2003). The classification for the biological processes that the 17 age-related NOS2-dependent SNO proteins were: metabolic processes (32.3%), cellular processes (29%), biological regulation (12.9%), localization (9.7%), multicellular organismal processes (3.2%), and response to stimulus (12.9%). Furthermore, the 5 NOS2-dependent SNO proteins that increased by genotype comparison showed an involvement of similar pathways: metabolic processes (30%), cellular processes (30%), biological regulation (10%), localization (10%), multicellular organismal processes (10%), and response to stimulus (10%). In both comparisons (age- and genotype-dependent), metabolic and cellular processes were the most affected.

Following this, all SNO proteins that increased in the age- and genotype-dependent comparison were classified by their molecular function. The candidate proteins in the age comparison were classified into the following: catalytic activity (53.8%), binding (15.4%), transporter activity (15.4%), translation regulator activity (7.7%), and structural molecule activity (7.7%). Similarly, when genotypes were compared, alterations in catalytic activity (33.3%), binding (33.3%) and transporter activity (33.3%) were the most influenced processes.

Synaptosomal S-nitrosylation in human specimen

Pairwise comparisons were performed between AD, MCI and healthy control groups (Fig. 6 and Table S3). After quality control, a total of 291 SNO proteins were identified in synaptosome fractions derived from AD brains compared to MCI brains. The comparison between MCI and control samples included 289 SNO proteins and between AD and control 295 proteins. Applying the same statistical analysis for human candidates as for murine proteins, 16 SNO proteins were significantly increased when AD was compared with MCI, 1 SNO protein was found to be elevated when MCI was compared with controls and 9 SNO proteins were increased in AD cases as compared with control brains (Tables S3 and S4). No SNO protein overlapped between all three pairwise comparisons. Three SNO proteins were significant and shown in both pairwise comparisons, AD group against MCI or against controls. These were myelin-oligodendrocyte glycoprotein (MOG), glutathione s-transferase Mu 3 (GSTM3), and four, and a half LIM domains protein 1 (FHL1).

Functional classification of nitrosylated human proteins

Functional classification of up-regulated human SNO proteins included candidates found in at least one pairwise comparison. Following this criterion, 23 synapto-SNO were classified by their biological processes using Uniprot/SwissProt database and molecular functions using Panther Gene Ontology (Figure S2 and Table S4). The biological processes included cellular process (27.8%), cellular component organization or biogenesis (13.9%), metabolic process (13.9%), multicellular organismal process (13.9%), developmental process (11%), biological regulation (8.3%), immune system process (5.6%), localization (2.8%), and response to stimulus (2.8%). Subsequently, the analysis was done for their molecular function. The increase in human proteins was classified into the following: catalytic activity (30.7%), structural molecule activity (23.1%), binding (23.1%), signal transducer activity (7.7%), receptor activity (7.7%), and transporter activity (7.7%).

Discussion

Our proteomic study was designed to identify endogenous synaptic S-nitrosylated (synapto-SNO) proteins in murine and human synaptosomes. In order to assess the contribution

Table 2 List of NOS2-dependent synapto-SNO proteins increased in aging and/ or APP/PS1 genotype mice

Protein name	Swiss-prot ID	Gene	Peptide sequence	SNO pos. (aa)	Factor	Fold change	Bootstrap 95% CI	*p*-value Limma	*p*-value RP
Elongation factor 2	P58252	EEF2	STLTDSLV**C**K	41	Aging	1.2	Yes	0.25	0.52
Heme oxygenase 2	O70252	HMOX2	GTLGGSN**C**PFQTTVAVLR	281*	Aging	1.2	Yes	0.35	0.34
Succinate dehydrogenase [ubiquinone] flavoprotein subunit, mitochondria	Q8K2B3	SDHA	AAFGLSEAGFNTA**C**LTK	89	Aging	1.2	Yes	0.19	0.38
Excitatory amino acid transporter 1	P56564	SLC1A3	**C**LEENNGVDKR	375*	Aging	1.2	Yes	0.25	0.37
					APP/PS1 – WT	1.2	Yes	0.99	0.73
					APP/PS1 – ANO	1.3	Yes	0.72	0.45
Phospholipid phosphatase 3	Q99JY8	PLPP3	GFY**C**NDESIK	68*	Aging	1.3	Yes	0.18	0.35
Zinc transporter 3	P97441	SLC30A3	LEGMAFHH**C**HK	55*	Aging	1.3	Yes	0.30	0.46
CLIP-associating protein 2	Q8BRT1	CLASP2	SLLVAGAAQYD**C**FFQHLR	135*	Aging	1.3	Yes	0.40	0.58
Succinyl-CoA ligase [ADP-forming] subunit beta, mitochondrial	Q9Z2I9	SUCLA2	I**C**NQVLV**C**ER	152 or 158	Aging	1.3	Yes	0.06	0.38
Acyl carrier protein, mitochondrial	Q9CR21	NDUFAB1	LM**C**PQEIVDYIADK	140	Aging	1.4	Yes	0.19	0.59
					APP/PS1 – WT	1.2	Yes	0.99	0.73
					APP/PS1 – ANO	1.2	Yes	0.91	0.69
					Aging	1.3	Yes	0.29	0.54
Sodium/potassium-transporting ATPase subunit alpha-3	Q6PIC6	ATP1A3	SSHTWVALSHIAGL**C**NR	418	Aging	1.3	yes	0.41	0.27
Inactive hydroxysteroid dehydrogenase-like protein 1	Q8BTX9	HSDL1	**C**PWLAPSPR	265*	Aging	1.3	Yes	0.18	0.34
					APP/PS1 – WT	1.2	Yes	0.99	0.73
					APP/PS1 – ANO	1.4	Yes	0.72	0.45
Succinyl-CoA:3-ketoacid coenzyme A transferase 1, mitochondrial	Q9D0K2	OXCT1	STG**C**DFAVSPN	504	Aging	1.3	Yes	0.13	0.22
Receptor-type tyrosine-protein phosphatase alpha	P18052	PTPRA	TGTF**C**ALSTVLER	770*	Aging	1.4	Yes	0.19	0.48
NFU1 iron–sulfur cluster scaffold homolog, mitochondrial	Q9QZ23	NFU1	LQGS**C**TS**C**PSSIITLK	210 or 213*	Aging	1.4	Yes	0.05	0.38
Protein NDRG2	Q9QYG0	NDRG2	**C**PVMLVVGDQAPHEDAVVE**C**NSK	255 and 274	Aging	1.5	Yes	0.23	0.38
					APP/PS1 – WT	1.3	Yes	0.99	0.73
					APP/PS1 – ANO	1.2	Yes	0.91	0.74
AP-2 complex subunit beta	Q9DBG3	AP2B1	E**C**HLNADTVSSK	857	Aging	1.7	Yes	0.08	0.42
Pyruvate carboxylase, mitochondrial	Q05920	PC	FLYE**C**PWR	622	Aging	1.7	Yes	0.03	0.03
Alcohol dehydrogenase class-3	P28474	ADH5	F**C**LNPK	103	APP/PS1 – WT	1.4	Yes	0.99	0.73
					APP/PS1 – ANO	1.6	Yes	0.72	0.69

Positions of the SNO site refer to the canonic Swiss-Prot sequences. Asterisks indicate proteins that have not been reported in previous nitrosylation studies according to a nitrosylation database (Lee *et al.* 2012b). "Factor" describes the comparison in which the protein was identified, either based on aging or APP/PS1 genotype (NOS2 dependent). For proteins found in both aging and genotype conditions, respective fold changes and significance measures are listed ($p < 0.05$).

of NOS2-induced neuroinflammation in the pathogenesis of AD, a NOS2-deficient mouse model was used. An optimized protocol for mass spectrometry-based proteomics, using iodoTMT^{TM} isobaric tag labeling was applied to identify synapto-SNO protein modifications during physiological aging and along the AD trajectory. The performance of this protocol was comparable to our previous results (Wijasa *et al.* 2017).

S-nitrosylation is a fragile modification with fast turnover, although the SNO stability can vary between different proteins (Paige *et al.* 2008). Currently, there is no established method for "fixation" of SNO, resulting in potential loss of SNO during sample preparation steps such as isolation of the synaptosomes. The protocol applied in this study includes physical and chemical measures to reduce this loss, such as cooling and light protection, and exclusion of substances with known SNO-modifying properties such as thiol blockers. Nonetheless, the identified SNO proteins should be considered as a fraction of the "true" SNO proteome of synapses, potentially representing those nitrosylation sites in synaptic proteins that are most stable. On the other hand, such stable SNO sites could even be advantageous for biomarker discovery approaches. In general, the protocol applied in this study yields good comparability when compared to other studies on the synaptic proteome. Nevertheless, only a small overlap was found between the identified proteins and other studies on the SNO-proteome (Seneviratne *et al.* 2016; Amal *et al.* 2019). Yet, these studies analyzed whole-brain regions utilizing different models and enrichment strategies for nitrosylated peptides. Further improvement of techniques for SNO characterization is still desirable to reduce such limitations.

Quantitative proteome analysis of multiple non-identical data sets can be challenging due to missing values (Nilsson *et al.* 2010; Schwammle *et al.* 2013). To overcome this limitation, this study applied a combination of Limma, RP, and bootstrap analyses. Limma and RP are well-established methods for statistical analysis of large data sets that contain missing values, but are still robust enough to prevent the false positive (type I error) data estimations (Mukherjee *et al.* 2003; Schwammle *et al.* 2013). The bootstrap method, however, provides more accurate family wise error rate/FWER (probability of making false discovery or type 1 error) and introduces fewer type 2 errors (false negative) compared with standard methods (e.g., Bonferroni's correction) for multiple comparison analyses (Dudoit *et al.* 2004; Forrest *et al.* 2005; Søgaard *et al.* 2014). Their combined usage is complementary and yields high detection rates of regulated features (du Prel *et al.* 2009).

Biologically, various mechanisms may cause the differences of synapto-SNO protein levels observed in the present study. Changes in protein expression prior to nitrosylation (Hong *et al.* 2009; Papuc´ *et al.* 2015), increased NOS2 activity (Chen *et al.* 2012; Heneka *et al.* 2015) or other NO sources such as from food and drugs may account for the altered s-nitrosylation of the synaptosome (Ahmad 1995; Nakamura *et al.* 2013; Al-Gubory 2014; Faraco *et al.* 2014), limiting the interpretation of the obtained results. Another factor that increases the production of NO is oxidative stress, which is implicated in the natural aging process as well as a variety of disease states (Tonnies and Trushina 2017).

To identify those synapto-SNO proteins most likely related to inflammation-induced NOS2 activation, this study focused on the up-regulated SNO proteins identified from mouse and human synaptosomes, as the induction of NOS2 expression and subsequent NO generation is likely to increase SNO. The mouse models furthermore included NOS2 KO mice, enabling elimination of those protein candidates that were NOS2 independent and unlikely to be related to inflammatory reactions. Mouse data analysis was performed for age-associated and genotype-mediated effects. S-nitrosylation of synaptosomes derived from 3-month-old WT animals was compared with 12-month-old WT mice, revealing an increase in S-nitrosylated proteins during physiological aging. In contrast, age-associated effects observed in APP/PS1 mice were interpreted as pathological aging, in which increases in SNO were related to Aβ deposition and neuroinflammation.

Based on analysis of the mice data set, there were 18 NOS2-dependent synapto-SNOs that increased as a result of age and/ or APP/PS1 genotype (Table 2 and Fig. 4). Most of these proteins were involved in metabolic processes (figure 5), supporting previous findings on alterations of metabolic pathways in AD that may contribute to the development of neurological symptoms (Cai *et al.* 2012; Kaddurah-Daouk *et al.* 2013; Trushina *et al.* 2013). In a similar manner, several synapto-SNOs could be attributed to the regulation of cell growth, cell cycle, cell division, cell communication, and cell death (Bult *et al.* 2008). The most relevant candidates comprise seven proteins that were either changed in NOS2-dependent manner in the APP/PS1 animals (ADH5), in NOS2/ APP/PS1/ age-dependent manner (SLC1A3, NDUFAB1, HSDL1, NDRG2) or age-dependent and relevant for synaptic function (EEF2, SLC30A3, SLC1A3).

Three of these proteins (NDRG2, HSDL1 and ADH5) have been previously associated with pathophysiological aging. NDRG2 is a cytoplasmic protein involved in cell differentiation and is mainly expressed by astrocytes (Breuer *et al.* 2013). NDRG2 may function in synapse formation, neural differentiation, and axon survival in response to glucocorticoids (Deng *et al.* 2003; Nichols *et al.* 2005). Prior studies confirmed the increase of NDRG2 levels in AD dystrophic neurons and senile plaques (Mitchelmore *et al.* 2004) as well as APP/PS1 transgenic mice brains (Rong *et al.* 2017). The SNO sites described in this study (amino acid position 255 and 274) have been previously identified in an experiment utilizing induced nitrosylation, but the functional consequences of these modifications are unknown (Kohr *et al.* 2012). To our knowledge, there is no report on levels of

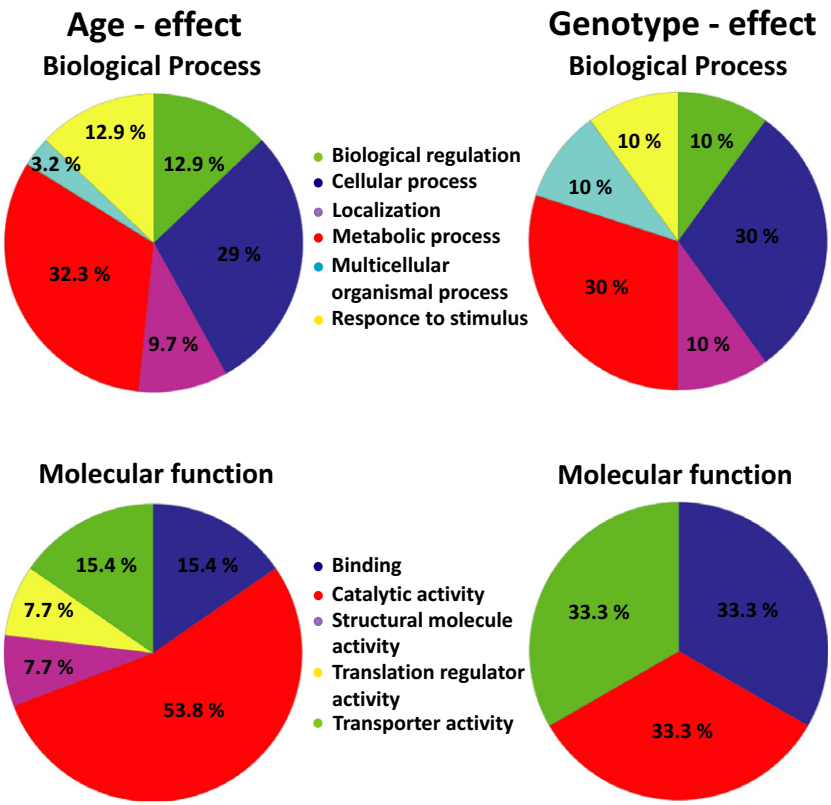

Fig. 5 Functional classification of regulated SNO proteins in murine synaptosomes. Functional categories were based on the annotations of Gene Ontology using the PANTHER Classification System for the categories of biological processes and molecular functions.

NDRG2 in cerebrospinal fluid or other AD-relevant biofluids that could serve as biomarker resource. Potentially, dystrophic neurons/ synapses could release this protein (or its nitrosylated variant), making it a potential target for validation.

HSDL1, identified for the first time as nitrosylated in this study, is a barely investigated protein. Its original enzymatic center is inactive due to conserved amino acid exchanges, although it appears to retain other functions (Meier *et al.* 2009). To our knowledge, there is no data on its potential role in synapses or even the central nervous system itself. ADH5, an alcohol dehydrogenase predominantly found in the liver, has been detected in lower amounts in mitochondria and in the hippocampus of AD patients, potentially explaining its identification in synaptosomes (Zhang *et al.* 2015; Guebel and Torres 2016). Yet, which particular functions this enzyme would have in a synapse is unknown. HSDL1 and ADH5 therefore constitute less promising biomarker candidates.

More interestingly, NDUFAB1 (subunit complex I of the mitochondrial respiratory chain) and SDHA (subunit complex II of the mitochondrial respiratory chain) have been previously associated with several neurodegenerative disease. This study identified both proteins as NOS2-dependent synapto-SNO proteins that increased during aging in APP/PS1 mice. NDUFAB1 regulation was previously related to aging and has been shown to be responsible for oxidative phosphorylation and down-regulated in AD patients (Kim *et al.* 2001; Mayer *et al.* 2018; Akila Parvathy Dharshini *et al.* 2019). NDUFAB1 reduction may lead to energy metabolism impairment and result in neuronal cell death by apoptosis (Kim *et al.* 2001). This study identified an SNO site at position 140 in the amino acid sequence that has been found in previous studies both under artificial as well as basal conditions, but the precise effects of the nitrosylation remain unclear (Kohr *et al.* 2011; Kohr *et al.* 2012). SDHA in turn contributes to nervous system development and was found to be nitrosylated–at the amino acid position 89 identified in this study–in neuropathic pain as well as under artificial conditions (Scheving 2013). Oxidative stress induces the increase in SDHA expression in the brain of AD patients (Bubber *et al.* 2005; Shi and Gibson 2011). Thus, nitrosylated NDUFAB1 and SDHA may be of interest for mechanistic studies and – if released from degenerating synapses – as potential biomarker candidates.

Another three of the "top 7" proteins – SLC1A3, SLC30A3 and EEF2 – are involved in synapse function: SLC1A3 or excitatory amino acid transporter 1 (EEAT1) plays an important role for neurotransmission and glutamate uptake (Bateman *et al.* 2015). SLC1A3/EEAT1 is strongly expressed by cortical neurons in AD cases (Scott *et al.* 2002). SLC30A3 or ZnT3, a zink transporter, is highly expressed on synaptic vesicle membranes and is involved in zinc accumulation in synaptic vesicles (Cole *et al.* 1999). Previous studies found a decrease in SLC30A3 protein levels in the

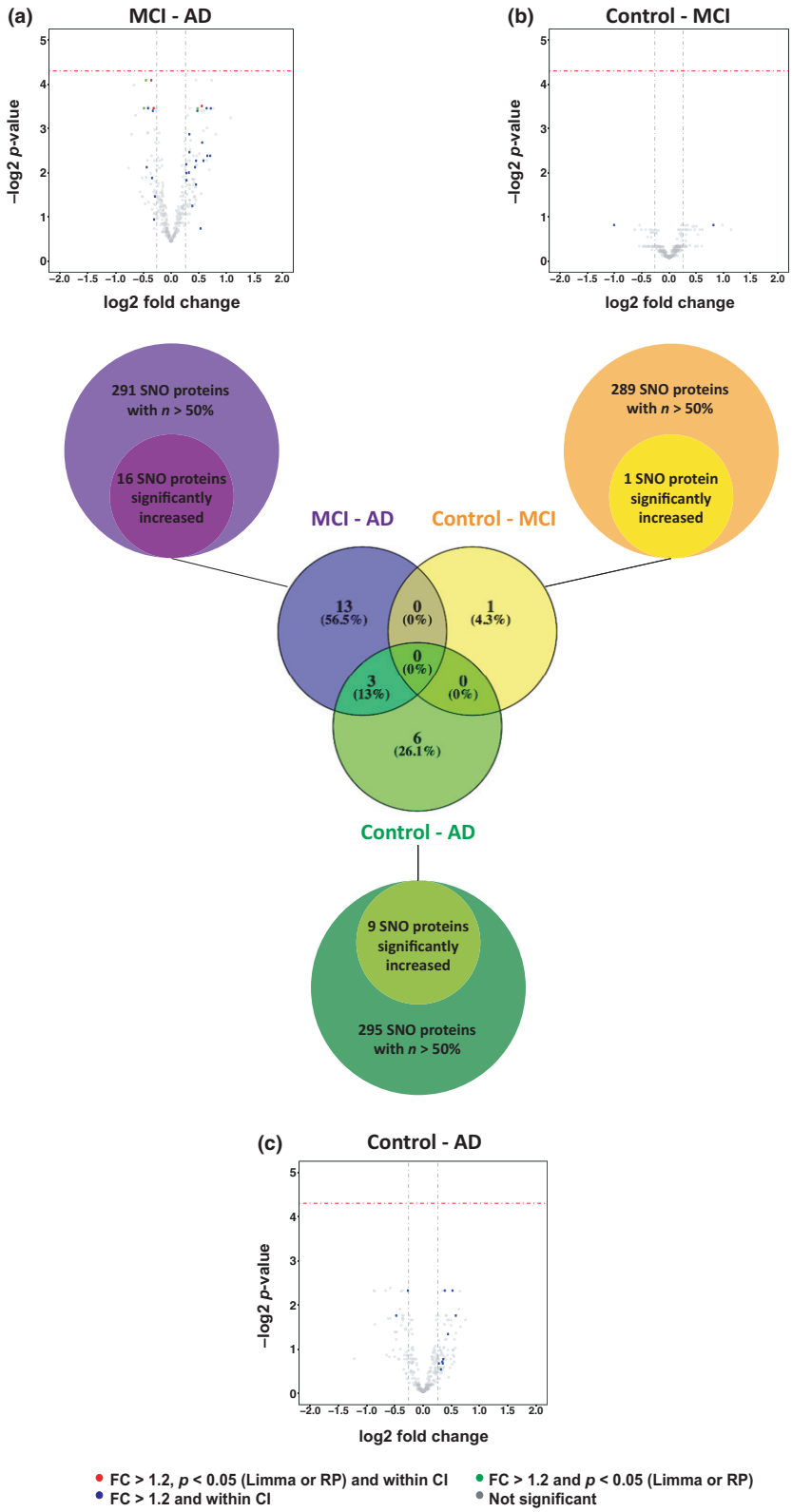

Fig. 6 Distribution of proteomics data from human specimen. Representative of synapto-SNO-proteome data were processed and analyzed for the comparison between cohorts of human patients. (a) The comparison of AD vs. MCI samples included 291 SNO proteins. Of these, 16 proteins were significantly up-regulated). (b) MCI vs. control samples (289 SNO proteins included, only one protein significantly up-regulated). (c) AD vs. controls (295 SNO proteins included, 9 proteins up-regulated). The most significant proteins were found comparing AD to MCI patients or AD patients to controls, with little overlap between these data sets. In volcano plots, negative $\log_2$ p-values (adjusted Limma p) were plotted against $\log_2$ protein fold change values. Dotted lines indicate the minimum fold change (grey lines) and p-values (orange) considered significant.

prefrontal AD cortex (Beyer *et al.* 2009; Kurita *et al.* 2016) and Tg2576 mice (Lee *et al.* 2012a). Both SLC1A3 and SLC30A3 have not been described as nitrosylated before. They constitute multi-pass transmembrane proteins with potentially limited solubility outside the membrane lipid bilayer, limiting their potential for use as biomarkers.

EEF2 is a main regulator for synaptic plasticity, memory consolidation and its level significantly reduced in AD patients (Li *et al.* 2005; Garcia-Esparcia *et al.* 2017) and also in old APP/PS1 transgenic mice (Garcia-Esparcia *et al.* 2017). Our result show that EEF2, nitrosylated in a NOS2-dependant manner, is increased in aged APP/PS1 transgenic mice. Although elongation factors are traditionally thought of as nuclear components and EEF is indeed an important sensor for synaptic signaling induced translation in neurons, it has also been shown to be localized in dendrites, nerve growth cones and in postsynaptic local translation sites (Asaki *et al.* 2003; Sutton *et al.* 2007; Iizuka *et al.* 2007; Heise *et al.* 2014). The nitrosylation site of EEF2 on amino acid position 41 appears to be relatively stable (persistent under biological conditions) and was identified in multiple previous publications, including another study on synaptosomes from the APP transgenic APPV717I AD mouse model (Paige *et al.* 2008; Doulias *et al.* 2010; Chen *et al.* 2010; Kohr *et al.* 2011; Kohr *et al.* 2012; Zareba-Koziol *et al.* 2014). These findings indicate a reproducible and stable modification, which would be advantageous for further investigations.

The number of identified S-nitrosylated proteins was considerably lower in human than in murine brain samples. This may have been caused by differences of pre-analytical sample handling and processing. In contrast to mouse brain sampling, which was performed in highly controlled and defined conditions, human brain tissue was taken after variable post-mortem intervals. Although the post-mortem interval was limited to 4 h for this study, the total levels of protein SNO may have decreased and this may have limited the overall yield in human samples (Zareba-Koziol *et al.* 2014). One way to reduce such limitations in the future are rapid autopsy programs for AD cases, designed to enable the analysis of labile post-translational modifications (i.e., Rapid Autopsy Program of the University Alzheimer's Disease Reseach Center, UKADRC) (Schmitt *et al.* 2012).

Despite these limitations, the human study identified 23 synapto-SNO proteins as potential candidate biomarkers (Table S4). Three synapto-SNO proteins (MOG, FHL1 and GSTM3) were found to increase in AD compared to both MCI and control subjects. Nitrosylations on MOG and FHL1 were identified for the first time. MOG is a myelin component, which is expressed at the oligodendrocyte plasma membrane and outer surface of the myelin sheath (Brunner *et al.* 1989; Bateman *et al.* 2015). Papuc´ et al. showed significantly increased production of autoantibodies against MOG protein in AD, indicating early demyelination of the hippocampal region (Papuc´ *et al.* 2015). While biomarker approaches are focusses on detection of autoantibodies against MOG, the protein or its nitrosylated variant could be released during demyelination and constitute a biomarker candidate on its own.

FHL1 is expressed mainly in the cardiac, skeletal muscle and brain (Lee *et al.* 1998). The spliced variant named FHL1B is specifically expressed in brain and probably related to neural differentiation, inflammatory response and certain fragile X syndrome (Lee *et al.* 1999; Zhang *et al.* 2018). FHL1 gene mutations result in chronic myopathies, which are characterized by an accumulation of aggregated proteins and vacuoles filled with misfolded proteins (Sabatelli *et al.* 2014). The precise functions of FHL1 in synapses are unclear. GSTM3 is a cytoplasmic protein that belongs to the glutathione S-transferase superfamily. GSTM3 has been described to protect cells from the oxidative stress. In addition, it has been found at sites of Aβ deposition and in microglia of AD brains (Tchaikovskaya *et al.* 2005). The nitrosylation of GSTM3 at position 3 has been previously described in a methods study on SNO-protein enrichment (Forrester *et al.* 2009), but there is little data on the function of this protein specifically in neurons or synapses. As cytosolic proteins, both FHL1 and GSTM3 could remain soluble after release from dystrophic synapses and constitute potential biomarker candidates.

The human candidate list also included proteins previously described to be involved in AD pathophysiology: Neurocan core protein (NCAN), calmodulin-dependent protein kinase type II subunit gamma (CAMK2G), CD44 and aspartate aminotransferase (GOT1). Importantly, all of these 4 proteins have been previously detected in CSF, which is a promising prerequisite for further biomarker research using these candidates:

NCAN is a secreted protein that is involved in central nervous system development. To our knowledge, there are no previous studies describing a nitrosylation site on NCAN. It is an extracellular matrix component and involved in synapse formation and stabilization (Besson *et al.* 2015; Sethi and Zaia 2017). The protein itself has already been described as potential synaptic biomarker in the CSF of patients with MCI progressing to AD dementia, and has also been related to schizophrenia (Sethi and Zaia 2017; Duits *et al.* 2018). It therefore constitutes a quite reasonable candidate for further characterization.

CAMK2G is found on the cytoplasmic side of the cell membrane. In neurons, it may participate in synapse formation, maintenance of synaptic plasticity that enables long-term potentiation (LTP) and hippocampus-dependent learning (Lisman *et al.* 2002; Rose *et al.* 2006). It has been suggested to be a toxicity modulator in Alzheimer's disease (Ghosh and Giese 2015). RNA expression of CAMK2G is altered in AD blood versus control (Bai *et al.* 2014). Noteworthy, CAMK2G expression is also altered in brain tissue of TREM2 KO mice, linking it to the most prominent immune gene risk factor for AD (Carbajosa *et al.* 2018). Altered CAMK2 levels have been found in glioblastoma biopsies and it was detectable by mass spectrometry in CSF (Polisetty *et al.* 2012). CAMK2G has not been described as

nitrosylated before, but it is given detectability in CSF making it a promising candidate.

CD44 is a cell surface glycoprotein protein that is broadly expressed on immune cells and may act as an adhesion molecule for astrocytes (Akiyama *et al.* 1993; Mak and Saunders 2006). It is also localized at dendrites and synapses and might be involved in synaptic plasticity, neuronal development and neurodegeneration (Mak and Saunders 2006; Roszkowska *et al.* 2016) and was described in CSF in example in studies on depression or Lyme disease, increasing its biomarker potential (Ditzen *et al.* 2012; Angel *et al.* 2012). The AD related secretases Presenilin and γ-secretase cleave CD44, which is a single-pass transmembrane receptor (Wolfe 2007). Like NCAN and CAMK2G, it was not described as nitrosylated before but could provide a detectable biomarker candidate.

GOT1 is localized in the cytoplasm and acts as a scavenger of glutamate in brain neuroprotection. To our knowledge, there is only scarce data on its specific functions in neurons or synapses, but GOT1 activity was found to be increased in CSF (D'Aniello *et al.* 2005) and urine (Watanabe *et al.* 2019) of patients with Alzheimer disease compared to controls. The SNO site described in this study on position 46 of the human sequence has been previously found in a technical setting (Forrester *et al.* 2009). Like the other human candidate proteins in focus, GOT1 therefore holds biomarker potential.

In summary, this is the first study that investigated the APP/PS1 murine and the AD spectrum human synaptic nitroso-proteome under physiological and pathological conditions with focus on inflammation-induced changes. Further studies, in particular large-scale CSF studies, of the most promising candidate proteins (EEF2, NDUFAB1, NDRG2, MOG, FHL1, GSTM3, NCAN, CAMK2G, CD44, and GOT1) are required to validate the findings and evaluate their potential as early biomarkers for AD.

Acknowledgments and conflict of interest disclosure

This work was supported in the frame of the BIOMARKAPD (01ED1203B) project within the EU Joint Programs for Neurodegenerative Diseases Research (JPND), the European Union's Seventh Framework Programme (FP7/2007-2013) under grant agreement n° HEALTH-F2-2011-278850 (INMiND) and the EU-IMI program n° 115568 (AETIONOMY). Michael T. Heneka is a member of the Cluster of Excellence "Immunosensation". The Banner Sun Health Research Institute Brain and Body Donation Program is supported by the National Institute of Neurological Disorders and Stroke, U24 NS072026 National Brain and Tissue Resource for Parkinson's Disease and Related Disorders; National Institute on Aging, P30 AG19610 Arizona Alzheimer's Disease Core Center; Arizona Department of Health Services, Arizona Alzheimer's Consortium; Arizona Biomedical Research Commission, Arizona Parkinson's Disease Consortium; Michael J. Fox Foundation for Parkinson's Research. Thanks to Dr. Elizabeth Campbell and Dr. Roisin McManus for proofreading the article. MTH holds editorship at the Journal of Neurochemistry.

All experiments were conducted in compliance with the ARRIVE guidelines.

Authors contribution

TSW performed initial testing experiments, animal, and human brain preparations, synaptosome isolation, protein labeling, data analysis, and drafted the manuscript, MS performed the mass spectrometric measurements and MS data analysis, FS performed the western blot and immunoprecipitation, FB, and MTH designed the study, supervised experiments and interpretation, and drafted the manuscript, VG approved the study and drafted the manuscript.

Supporting information

Additional supporting information may be found online in the Supporting Information section at the end of the article.

Figure S1. Immunoblot analysis of synaptosome enrichment.

Figure S2. Functional classification of upregulated SNO proteins in human synaptosomes.

Table S1. Statistical analyses of age-dependent effects in mouse synaptosomes.

Table S2. Statistical analyses of genotype-dependent effects in mouse synaptosomes

Table S3. Disease-stage dependent comparison of human proteome data.

Table S4. Synapto-SNO proteins increased in human AD samples.

References

Agostinho P., Cunha R. A. and Oliveira C. (2010) Neuroinflammation, oxidative stress and the pathogenesis of Alzheimer' s disease. *Curr. Pharm. Des.* **16**, 2766–2778.

Ahmad S. (1995) Oxidative stress from environmental pollutants. *Arch Insect Biochem Physiol.* **29**, 135–157.

Akila Parvathy Dharshini S., Taguchi Y. -H. and Michael Gromiha M. (2019) Exploring the selective vulnerability in Alzheimer disease using tissue specific variant analysis. *Genomics* **111**, 936–949.

Akiyama H., Tooyama I., Kawamata T., Ikeda K. and McGeer P. L. (1993) Morphological diversities of CD44 positive astrocytes in the cerebral cortex of normal subjects and patients with Alzheimer's disease. *Brain Res.* **632**, 249–259.

Al-Gubory K. H. (2014) Environmental pollutants and lifestyle factors induce oxidative stress and poor prenatal development. *Reprod Biomed Online* **29**, 17–31.

Amal H., Gong G., Gjoneska E., Lewis S. M., Wishnok J. S., Tsai L.-H. and Tannenbaum S. R. (2019) S-nitrosylation of E3 ubiquitin-protein ligase RNF213 alters non-canonical Wnt/Ca+2 signaling in the P301S mouse model of tauopathy. *Transl. Psychiatry* **9**, 1–12.

Angel T. E., Jacobs J. M., Smith R. P., *et al.* (2012) Cerebrospinal fluid proteome of patients with acute Lyme disease. *J. Proteome Res.* **11**, 4814–4822.

Asaki C., Usuda N., Nakazawa A., Kametani K. and Suzuki T. (2003) Localization of translational components at the ultramicroscopic level at postsynaptic sites of the rat brain. *Brain Res.* **972**, 168–176.

Bai Z., Stamova B., Xu H., *et al.* (2014) Distinctive RNA expression profiles in blood associated with Alzheimer disease after accounting for white matter hyperintensities. *Alzheimer Dis. Assoc. Disord.* **28**, 226–233.

Bateman A., Martin M. J., O'Donovan C., *et al.* (2015) UniProt: A hub for protein information. *Nucleic Acids Res.* **43**, D204–D212.

Beach T. G., Adler C. H., Sue L. I., *et al.* (2015) Arizona study of aging and neurodegenerative disorders and brain and body donation program. *Neuropathology* **35**, 354–389.

Besson F. L., La Joie R., Doeuvre L., *et al.* (2015) Cognitive and brain profiles associated with current neuroimaging biomarkers of preclinical Alzheimer's disease. *J. Neurosci. Off. J. Soc. Neurosci.* **35**, 10402–10411.

Beyer N., Coulson D. T. R., Heggarty S., Ravid R., Irvine G. B., Hellemans J. and Johnston J. A. (2009) ZnT3 mRNA levels are reduced in Alzheimer's disease post-mortem brain. *Mol. Neurodegener.* **4**, 53.

Blonder J. and Veenstra T. D. (2007) Computational prediction of proteotypic peptides. *Expert Rev Proteomics. Expert Rev Proteomics* **4**, 351–354.

Boyd-Kimball D., Castegna A., Sultana R., Poon H. F., Petroze R., Lynn B. C., Klein J. B. and Butterfield D. A. (2005) Proteomic identification of proteins oxidized by Abeta(1–42) in synaptosomes: implications for Alzheimer's disease. *Brain Res.* **1044**, 206–15.

Breuer K., Foroushani A. K., Laird M. R., Chen C., Sribnaia A., Lo R., Winsor G. L., Hancock R. E. W., Brinkman F. S. L. and Lynn D. J. (2013) InnateDB: systems biology of innate immunity and beyond—recent updates and continuing curation. *Nucl. Acids Res.* **41**, 1228–1233.

Brunner C., Lassmann H., Waehneldt T. and Matthieu J. M. (1989) Differential ultrastructural localization of myelin basic pro- tein, myelin/oligodendroglial glycoprotein, and 2′,3′-cyclic nucleotide 3′-phosphodiesterase in the CNS of adult rats. *J. Neurochem.* **52**, 296–304.

Bubber P., Haroutunian V., Fisch G., Blass J. P. and Gibson G. E. (2005) Mitochondrial abnormalities in Alzheimer brain: mechanistic implications. *Ann. Neurol.* **57**, 695–703.

Bult C. J., Eppig J. T., Kadin J. A., Richardson J. E. and Blake J. A. and the members of the Mouse Genome Database Group (2008) The mouse genome database (MGD): mouse biology and model systems. *Nucleic Acids Res* **36**, D724–728.

Cai H., Cong W., Ji S., Rothman S., Maudsley S. and Martin B. (2012) Metabolic dysfunction in Alzheimer's disease and related neurodegenerative disorders. *Curr Alzheimer Res.* **9**, 5–17.

Carbajosa G., Malki K., Lawless N., *et al.* (2018) Loss of Trem2 in microglia leads to widespread disruption of cell coexpression networks in mouse brain. *Neurobiol. Aging* **69**, 151–166.

Chang R. Y. K., Nouwens A. S., Dodd P. R. and Etheridge N. (2013) The synaptic proteome in Alzheimer's disease. *Alzheimers Dement. J. Alzheimers Assoc.* **9**, 499–511.

Chen Y.-J., Ku W.-C., Lin P.-Y., Chou H.-C., Khoo K.-H. and Chen Y.-J. (2010) S-alkylating labeling strategy for site-specific identification of the s-nitrosoproteome. *J. Proteome Res.* **9**, 6417–6439.

Chen X., Guan T., Li C., Shang H., Cui L., Li X.-M. and Kong J. (2012) SOD1 aggregation in astrocytes following ischemia/reperfusion injury: a role of NO-mediated S-nitrosylation of protein disulfide isomerase (PDI). *J. Neuroinflammation* **9**, 237–237.

Cole T. B., Wenzel H. J., Kafer K. E., Schwartzkroin P. A. and Palmiter R. D. (1999) Elimination of zinc from synaptic vesicles in the intact mouse brain by disruption of the ZnT3 gene. *Proc. Natl Acad. Sci. USA* **96**, 1716–1721.

Colton C. A., Wilcock D. M., Wink D. A., Davis J., Van W. E. and Vitek M. P. (2008) The Effects of NOS2 gene deletion on mice expressing mutated human AβPP. *J. Alzheimer Dis.* **15**, 571–587.

D'Aniello A., Fisher G., Migliaccio N., Cammisa G., D'Aniello E. and Spinelli P. (2005) Amino acids and transaminases activity in ventricular CSF and in brain of normal and Alzheimer patients. *Neurosci. Lett.* **388**, 49–53.

Davies C. A. A., Mann D. M. A. M., Sumpter P. Q. Q. and Yates P. O. O. (1987) A quantitative morphometric analysis of the neuronal and synaptic content of the frontal and temporal cortex in patients with Alzheimer's disease. *J. Neurol. Sci.* **78**, 151–164.

DeKosky S. T. and Scheff W. (1990) Synapse loss in frontal cortex biopsies in Alzheimer's disease: correlation with cognitve severity. *Ann. Neurol.* **27**, 457–464.

Deng Y., Yao L., Chau L., *et al.* (2003) N-Myc downstream-regulated gene 2 (NDRG2) inhibits glioblastoma cell proliferation. *Int. J. Cancer* **106**, 342–347.

Ditzen C., Tang N., Jastorff A. M., *et al.* (2012) Cerebrospinal fluid biomarkers for major depression confirm relevance of associated pathophysiology. *Neuropsychopharmacology* **37**, 1013–1025.

Doulias P.-T., Greene J. L., Greco T. M., Tenopoulou M., Seeholzer S. H., Dunbrack R. L. and Ischiropoulos H. (2010) Structural profiling of endogenous S-nitrosocysteine residues reveals unique features that accommodate diverse mechanisms for protein S-nitrosylation. *Proc. Natl Acad. Sci. USA* **107**, 16958–16963.

Dudoit S., Laan M. J. and van der Laan Mark J. (2004) Multiple testing. Part I. Single-step procedures for control of general type I error rates. *Stat. Appl. Genet. Mol. Biol.* **3**, 1–69.

Duits F. H., Brinkmalm G., Teunissen C. E., Brinkmalm A., Scheltens P., Van der Flier W. M., Zetterberg H. and Blennow K. (2018) Synaptic proteins in CSF as potential novel biomarkers for prognosis in prodromal Alzheimer's disease. *Alzheimers Res. Ther.* **10**, 5.

Eden E., Navon R., Steinfeld I., Lipson D. and Yakhini Z. (2009) GOrilla: a tool for discovery and visualization of enriched GO terms in ranked gene lists. *BMC Bioinformatics* **10**, 48.

Faraco G., Wijasa T. S., Park L., Moore J., Anrather J. and Iadecola C. (2014) Water deprivation induces neurovascular and cognitive dysfunction through vasopressin-induced oxidative stress. *J. Cereb. Blood Flow Metab. Off. J. Int. Soc. Cereb. Blood Flow Metab.* **34**, 1–9.

Fiandaca M. S., Mapstone M. E., Cheema A. K. and Federoff H. J. (2014) The critical need for defining preclinical biomarkers in Alzheimer ' s disease. *Alzheimers Dement.* **10**, S196–S212.

Forrest M. S., Lan Q., Hubbard A. E., *et al.* (2005) Discovery of novel biomarkers by microarray analysis of peripheral blood mononuclear cell gene expression in benzene-exposed workers. *Environ Health Perspect* **113**, 801–807.

Forrester M. T., Thompson J. W., Foster M. W., Nogueira L., Moseley M. A. and Stamler J. S. (2009) Proteomic analysis of S-nitrosylation and denitrosylation by resin-assisted capture. *Nat. Biotechnol.* **27**, 557–559.

Förstermann U. and Sessa W. C. (2012) Nitric oxide synthases: regulation and function. *Eur. Heart J.* **33**, 829–837.

Garcia-Esparcia P., Sideris-Lampretsas G., Hernandez-Ortega K., Grau-Rivera O., Sklaviadis T., Gelpi E. and Ferrer I. (2017) Altered mechanisms of protein synthesis in frontal cortex in Alzheimer disease and a mouse model. *Am. J. Neurodegener. Dis.* **6**, 15–25.

Ghosh A. and Giese K. P. (2015) Calcium/calmodulin-dependent kinase II and Alzheimer's disease. *Mol. Brain* **8**, 78.

Guebel D. V. and Torres N. V. (2016) Sexual dimorphism and aging in the human hyppocampus: identification, validation, and impact of differentially expressed genes by factorial microarray and network analysis. *Front. Aging Neurosci.* **8**, 229.

Hammerschmidt T., Kummer M. P., Terwel D., *et al.* (2013) Selective loss of noradrenaline exacerbates early cognitive dysfunction and synaptic deficits in APP/PS1 mice. *Biol. Psychiatry* **73**, 454–63.

Heise C., Gardoni F., Culotta L., Luca M., di Verpelli C.andSala C. (2014) Elongation factor-2 phosphorylation in dendrites and the regulation of dendritic mRNA translation in neurons. *Front. Cell Neurosci.* **8.**, 1–8.

Heneka M. T. and Feinstein D. L. (2001) Expression and function of inducible nitric oxide synthase in neurons. *J. Neuroimmunol.* **114**, 8–18.

Heneka M. T., Carson M. J., Khoury J. E., *et al.* (2015) Neuroinflammation in Alzheimer's disease. *Lancet Neurol.* **14**, 388–405.

Hong G.-S., Heun R., Jessen F., Popp J., Hentschel F., Kelemen P., Schulz A., Maier W. and Kölsch H. (2009) Gene variations in GSTM3 are a risk factor for Alzheimer's disease. *Neurobiol Aging* **30**, 691–696.

Iizuka A., Sengoku K., Iketani M., Nakamura F., Sato Y., Matsushita M., Nairn A. C., Takamatsu K., Goshima Y. and Takei K. (2007) Calcium-induced synergistic inhibition of a translational factor eEF2 in nerve growth cones. *Biochem. Biophys. Res. Commun.* **353**, 244–250.

Kaddurah-Daouk R., Zhu H., Sharma S., *et al.* (2013) Alterations in metabolic pathways and networks in Alzheimer's disease. *Transl Psychiatry.* **3**, e244.

Kim S. H., Vlkolinsky R., Cairns N., Fountoulakis M. and Lubec G. (2001) The reduction of NADH ubiquinone oxidoreductase 24- and 75-kDa subunits in brains of patients with Down syndrome and Alzheimer's disease. *Life Sci.* **68**, 2741–2750.

Kohr M. J., Aponte A. M., Sun J., Wang G., Murphy E., Gucek M. and Steenbergen C. (2011) Characterization of potential S-nitrosylation sites in the myocardium. *Am. J. Physiol. Heart Circ. Physiol.* **300**, H1327–1335.

Kohr M. J., Aponte A., Sun J., Gucek M., Steenbergen C. and Murphy E. (2012) Measurement of S-nitrosylation occupancy in the myocardium with cysteine-reactive tandem mass tags: short communication. *Circ. Res.* **111**, 1308–1312.

Kummer M. P., Hermes M., Delekarte A., *et al.* (2011) Nitration of tyrosine 10 critically enhances amyloid β aggregation and plaque formation. *Neuron* **71**, 833–44.

Kurita H., Okuda R., Yokoo K., Inden M. and Hozumi I. (2016) Protective roles of SLC30A3 against endoplasmic reticulum stress via ERK1/2 activation. *Biochem Biophys Res Commun.* **479**, 853–859.

Kuster B., Schirle M., Mallick P. and Aebersold R. (2005) Scoring proteomes with proteotypic peptide probes. *Nat. Rev. Mol. Cell Biol.* **6**, 577–583.

Lee S. M. Y., Tsui S. K. W., Chan K. K., Garcia-Barcelo M., Waye M. M. Y., Fung K. P., Liew C. C. and Lee C. Y. (1998) Chromosomal mapping, tissue distribution and cDNA sequence of Four-and-a-half LIM domain protein 1 (FHL1). *Gene* **216**, 163–170.

Lee S. M., Li H. Y., Ng E. K., *et al.* (1999) Characterization of a brain-specific nuclear LIM domain protein (FHL1B) which is an alternatively spliced variant of FHL1. *Gene* **237**, 253–263.

Lee J.-Y., Cho E., Seo J.-W., Hwang J. J. and Koh J.-Y. (2012a) Article navigation alteration of the cerebral zinc pool in a mouse model of Alzheimer disease. *J. Neuropathol. Exp. Neurol.* **71**, 211–222.

Lee T. Y., Chen Y. J., Lu C. T., Ching W. C., Teng Y. C., Huang H. and Da Chen Y. J. (2012b) dbSNO: A database of cysteine S-nitrosylation. *Bioinformatics* **28**, 2293–2295.

Li X., Alafuzoff I., Soininen H., Winblad B. and Pei J.-J. (2005) Levels of mTOR and its downstream targets 4E-BP1, eEF2, and eEF2 kinase in relationships with tau in Alzheimer's disease brain. *FEBS J.* **272**, 4211–4220.

Lisman J., Schulman H. and Cline H. (2002) The molecular basis of CaMKII function in synaptic and behavioural memory. *Nat. Rev. Neurosci.* **3**, 175–190.

Mak T. and Saunders M. (2006) The Immune Response - 1st ed.

Mallick P., Schirle M., Chen S. S., *et al.* (2007) Computational prediction of proteotypic peptides for quantitative proteomics. *Nat. Biotechnol* **25**, 125–131.

Mayer R. L., Schwarzmeier J. D., Gerner M. C., *et al.* (2018) Proteomics and metabolomics identify molecular mechanisms of aging potentially predisposing for chronic lymphocytic leukemia. *Mol. Cell. Proteomics MCP* **17**, 290–303.

Meier M., Tokarz J., Haller F., Mindnich R. and Adamski J. (2009) Human and zebrafish hydroxysteroid dehydrogenase like 1 (HSDL1) proteins are inactive enzymes but conserved among species. *Chem. Biol. Interact.* **178**, 197–205.

Meraz-Ríos M. A., Toral-Rios D., Franco-Bocanegra D., Villeda-Hernández J. and Campos-Peña V. (2013) Inflammatory process in Alzheimer's Disease. *Front. Integr. Neurosci.* **7**, 59–59.

Mitchelmore C., Büchmann-Møller S., Rask L., West M. J., Troncoso J. C. and Jensen N. A. (2004) NDRG2: a novel Alzheimer's disease associated protein. *Neurobiol Dis.* **16**, 48–58.

Mukherjee S. N., Sykacek P., Roberts S. J. and Gurr S. J. (2003) Gene ranking using bootstrapped *p*-values. *Sigkdd Explor.* **5**, 14–14.

Nakamura T., and Lipton S. A. (2016) Protein s-nitrosylation as a therapeutic target for neurodegenerative diseases. *Sci Trends Pharmacol* **37**, 73–84.

Nakamura T., Tu S., Akhtar M. W., Sunico C. R., Okamoto S.-I., and Lipton S. (2013) Aberrant protein s-nitrosylation in neurodegenerative diseases. *Neuron* **78**, 596–614.

Nichols N. R., Agolley D., Zieba M. and Bye N. (2005) Glucocorticoid regulation of glial responses during hippocampal neurodegeneration and regeneration. *Brain Res. Brain Res. Rev.* **48**, 287–301.

Nilsson T., Mann M., Aebersold R., Iii J. R. Y., Bairoch A. and Bergeron J. J. M. (2010) Mass spectrometry in high-throughput proteomics: ready for the big time. *Nat. Publ. Group* **7**, 681–685.

Paige J. S., Xu G., Stancevic B. and Jaffrey S. R. (2008) Nitrosothiol reactivity profiling identifies S-nitrosylated proteins with unexpected stability. *Chem. Biol.* **15**, 1307–1316.

Papuć E., Kurys-Denis E., Krupski W., Tatara M. and Rejdak K. (2015) Can antibodies against glial derived antigens be early biomarkers of hippocampal demyelination and memory loss in Alzheimer's disease? *Journal of Alzheimer's Disease* **48**, 115–121.

Polisetty R. V., Gautam P., Sharma R., *et al.* (2012) LC-MS/MS analysis of differentially expressed glioblastoma membrane proteome reveals altered calcium signaling and other protein groups of regulatory functions. *Mol. Cell. Prot.* **11**,1–15.

du Prel J.-B., Hommel G., Röhrig B. and Blettner M. (2009) Confidence interval or *p*-value?: part 4 of a series on evaluation of scientific publications. *Dtsch. Arzteblatt Int.* **106**, 335–339.

Rong X.-F., Sun Y.-N., Liu D.-M., Yin H.-J., Peng Y., Xu S.-F., Wang L. and Wang X.-L. (2017) The pathological roles of NDRG2 in Alzheimer's disease, a study using animal models and APPwt-overexpressed cells. *CNS Nerusci Ther* **23**, 667–679.

Rose A. J., Kiens B. and Richter E. A. (2006) Ca2+-calmodulin-dependent protein kinase expression and signalling in skeletal muscle during exercise. *J. Physiol.* **574**, 889–903.

Roszkowska M., Skupien A., Wójtowicz T., *et al.* (2016) CD44: a novel synaptic cell adhesion molecule regulating structural and functional plasticity of dendritic spines. *Mol. Biol. Cell* **27**, 4055–4066.

Sabatelli P., Castagnaro S., Tagliavini F., *et al.* (2014) Aggresome-autophagy involvement in a sarcopenic patient with rigid Spine syndrome and a p. C150R mutation in FHL1 gene. *Front. Aging Neurosci.* **6**, 215.

Scheving R. (2013) S-nitrosylation in Neuropathic pain and Autophagy.

Schmitt F. A., Nelson P. T., Abner E., *et al.* (2012) University of Kentucky Sanders-Brown healthy brain aging volunteers: donor characteristics, procedures, and neuropathology. *Curr. Alzheimer Res.* **9**, 724–733.

Schwammle V., Leon I. R. and Jensen O. N. (2013) Assessment and improvement of statistical tools for comparative proteomics analysis of sparse data sets with few experimental replicates. *J. Proteome Res.* **12**, 3874–3883.

Scott H., Pow D. V., Tannenberg A. E. G. and Dodd P. R. (2002) Aberrant expression of the glutamate transporter excitatory amino acid transporter 1 (EAAT1) in Alzheimer's disease. *J. Neurosci* **22**, RC206.

Seneviratne U., Nott A., Bhat V. B., Ravindra K. C., Wishnok J. S., Tsai L.-H. and Tannenbaum S. R. (2016) S-nitrosation of proteins relevant to Alzheimer's disease during early stages of neurodegeneration. *Proc. Natl Acad. Sci. USA* **113**, 4152–4157.

Sethi M. K. and Zaia J. (2017) Extracellular matrix proteomics in schizophrenia and Alzheimer's disease. *Anal. Bioanal. Chem.* **409**, 379–394.

Shi Q. and Gibson G. E. (2011) Up-regulation of the mitochondrial malate dehydrogenase by oxidative stress is mediated by miR-743a. *J. Neurochem.* **118**, 440–448.

Shi Z.-Q., Sunico C. R., McKercher S. R., Cui J., Feng G.-S., Nakamura T. and Lipton S. A. (2013) S-nitrosylated SHP-2 contributes to NMDA receptor- mediated excitotoxicity in acute ischemic stroke Zhong-Qing. *Proc. Natl Acad. Sci. USA* **110**, 3137–3142.

Søgaard A., Johannsen A., Plank B., Hovy D. and Martinez H. (2014) What's in a -value in NLP? In Proc. of CoNLL.

Sperling R. A., Aisen P. S., Beckett L. A., *et al.* (2011) Toward defining the preclinical stages of Alzheimer's disease: Recommendations from the National Institute on Aging-Alzheimer's Association workgroups on diagnostic guidelines for Alzheimer's disease. *Alzheimers Dement.* **7**, 280–292.

Sutton M. A., Taylor A. M., Ito H. T., Pham A. and Schuman E. M. (2007) Postsynaptic decoding of neural activity: eEF2 as a biochemical sensor coupling miniature synaptic transmission to local protein synthesis. *Neuron* **55**, 648–661.

Swomley A. M., Förster S., Keeney J. T., Triplett J., Zhang Z., Sultana R. and Butterfield D. A. (2014) Abeta, oxidative stress in Alzheimer disease: Evidence based on proteomics studies. *Biochim. Biophys. Acta* **1842**, 1248–1257.

Tchaikovskaya T., Fraifeld V., Urphanishvili T., Andorfer J. H., Davies P. and Listowsky I. (2005) Glutathione S-transferase hGSTM3 and ageing- associated neurodegeneration: relationship to Alzheimer's disease. *Mech. Mech Ageing Dev.* **126**, 309–315.

Terry R. D., Masliah E., Salmon D. P., Butters N., Deteresa R., Hill R., Hansen L. A. and Katzman R. (1991) Physical basis of cognitive alterations in Alzheimer ' s disease : Synapse loss is the major correlate of cognitive impairment. *Ann Neurol* **30**, 572–580.

Thomas P. D., Campbell M. J., Kejariwal A., Mi H., Karlak B., Daverman R., Diemer K., Muruganujan A. and Narechania A. (2003) PANTHER: A library of protein families and subfamilies indexed by function. *Genome Res.* **13**, 2129–2141.

Tomiyama T., Matsuyama S., Iso H., *et al.* (2010) A mouse model of amyloid beta oligomers: their contribution to synaptic alteration, abnormal tau phosphorylation, glial activation, and neuronal loss in vivo. *J. Neurosci. Off. J. Soc. Neurosci.* **30**, 4845–4856.

Tonnies E. and Trushina E. (2017) Oxidative stress, synaptic dysfunction, and Alzheimer's disease. *J. Alzheimer's Dis.* **57**, 1105–1121.

Trushina E., Dutta T., Persson X.-M. T., Mielke M. M. and Petersen Ronald C. (2013) Identification of altered metabolic pathways in plasma and CSF in mild cognitive impairment and Alzheimer's disease using metabolomics. *PLoS ONE* **8**, e63644.

Wang X., Anderson G. A., Smith R. D. and Dabney A. R. (2012) A hybrid approach to protein differential expression in mass spectrometry-based proteomics. *Bioinformatics* **28**, 1586–1591.

Watanabe Y., Hirao Y., Kasuga K., Tokutake T., Semizu Y., Kitamura K., Ikeuchi T., Nakamura K. and Yamamoto T. (2019) Molecular network analysis of the urinary proteome of Alzheimer's disease patients. *Dement. Geriatr. Cogn. Disord. Extra* **9**, 53–65.

Wijasa T. S., Sylvester M., Brocke-Ahmadinejad N., Kummer M. P., Brosseron F., Gieselmann V. and Heneka M. T. (2017) Proteome profiling of s-nitrosylated synaptosomal proteins by isobaric mass tags. *J. Neurosci. Methods* **291**, 95–100.

Wolfe M. S. (2007) When loss is gain: reduced presenilin proteolytic function leads to increased Aβ42/Aβ40. Talking Point on the role of presenilin mutations in Alzheimer disease. *EMBO Rep.* **8**, 136–140.

Yao P. J., Zhu M., Pyun E. I., Brooks A. I., Therianos S., Meyers V. E. and Coleman P. D. (2003) Defects in expression of genes related to synaptic vesicle trafficking in frontal cortex of Alzheimer's disease. *Neurobiol. Dis.* **12**, 97–109.

Zareba-Koziol M., Szwajda A., Dadlez M., Wyslouch-Cieszynska A. and Lalowski M. (2014) Global analysis of S-nitrosylation sites in the wild type (APP) transgenic mouse brain-clues for synaptic pathology. *Mol. Cell Proteomics* **13**, 2288–2305.

Zhang L., Guo X. Q., Chu J. F., Zhang X., Yan Z. R. and Li Y. Z. (2015) Potential hippocampal genes and pathways involved in Alzheimer's disease: a bioinformatic analysis. *Genet. Mol. Res.* **14**, 7218–7232.

Zhang W., Sun J., Cao H., Tian R., Cai L., Ding W. and Qian P.-Y. (2016) Post-translational modifications are enriched within protein functional groups important to bacterial adaptation within a deep-sea hydrothermal vent environment. *Microbiome* **4**, 49.

Zhang Q., Ma C., Gearing M., Wang P. G., Chin L.-S. and Li L. (2018) Integrated proteomics and network analysis identifies protein hubs and network alterations in Alzheimer's disease. *Acta Neuropathol. Commun.* **6**, 19.

